Chemical Physics 501 (2018) 121–127

Contents lists available at ScienceDirect

Chemical Physics

journal homepage: www.elsevier.com/locate/chemphys

Stretched-to-compressed-exponential crossover observed in the electrical degradation kinetics of some spinel-metallic screen-printed structures

V. Balitska [a], O. Shpotyuk [b,c,*], M. Brunner [d], I. Hadzaman [e]

[a] Lviv State University of Life Safety, 35, Kleparivska str., Lviv 79007, Ukraine
[b] Jan Dlugosz University in Czestochowa, 13/15, Armii Krajowej str., Czestochowa 4220, Poland
[c] Vlokh Institute of Physical Optics, 23, Dragomanov str., Lviv 79005, Ukraine
[d] Technische Hochschule Köln/University, Betzdorfer Strasse, Köln 50679, Germany
[e] Drohobych Ivan Franko State Pedagogical University, 24, I. Franko str., Drohobych 82100, Ukraine

ARTICLE INFO

Article history:
Received 24 November 2017
In final form 30 December 2017
Available online 2 January 2018

Keywords:
Electrical relaxation
Spinel
Ceramics
Kinetics
Stretched-exponential
Compressed-exponential

ABSTRACT

Thermally-induced (170 °C) degradation-relaxation kinetics is examined in screen-printed structures composed of spinel $Cu_{0.1}Ni_{0.1}Co_{1.6}Mn_{1.2}O_4$ ceramics with conductive Ag or Ag-Pd layered electrodes. Structural inhomogeneities due to Ag and Ag-Pd diffusants in spinel phase environment play a decisive role in non-exponential kinetics of negative relative resistance drift. If Ag migration in spinel is inhibited by Pd addition due to Ag-Pd alloy, the kinetics attains stretched exponential behavior with ~0.58 exponent, typical for one-stage diffusion in structurally-dispersive media. Under deep Ag penetration into spinel ceramics, as for thick films with Ag-layered electrodes, the degradation kinetics drastically changes, attaining features of two-step diffusing process governed by compressed-exponential dependence with power index of ~1.68. Crossover from stretched- to compressed-exponential kinetics in spinel-metallic structures is mapped on free energy landscape of non-barrier multi-well system under strong perturbation from equilibrium, showing transition with a character downhill scenario resulting in faster than exponential decaying.

1. Introduction

The stretched-exponential relaxation (SER) function (alternatively, nominated as *sub-exponential*) is most commonly used modelling curve to describe phenomenological response in degradation-relaxation (DR) kinetics in different substances prepared by freezing from a high-temperature out-of-equilibrium state [1–5]. In structurally-dispersive disordered solids, the tending towards equilibrium in the controlled parameter $\eta(t)$ occurs with increasingly slower DR rate, this process being known as physical aging (PhA) [6]. Deviation from simple single-exponential dependence (i.e. *non-exponentionality*) is defined by the Kohlrausch-Williams-Watts (KWW) functional [1,2]

$$\eta(t) \sim exp\left[-\left(\frac{t}{\tau}\right)^{\beta}\right], \quad (1)$$

where the time constant τ denotes *the relaxation time*, i.e. the characteristic time for the testing system to rearrange its structure towards an equilibrium, and *the dimensionless shape parameter* β (*non-exponentionality index* or *stretching exponent*) as an indicative of *wide distribution of diffusive relaxation times* attains positive less-unity values ($0 < \beta < 1$).

The KWW function (1) is not alone expression describing DR kinetics in different *out-of-equilibrium substances*. In a wide range of so-called *jammed systems* (including soft colloidal fractal gels, concentrated emulsions, surfactant phases, micellar polycrystals, lamellar gels, polymer nanocomposites [7–13], and even hard far-from-equilibrium metallic glasses [14,15]), where the initial relaxation concerns arrested diffusive motion typical for structurally dispersive solids, the final decay attains an unusual *compressed exponential relaxation* (CER) form, that can be explained by ultraslow ballistic motion of scatters under the action of internal stresses. Within this unusual CER kinetics (termed also as *squeezed-exponential* or *super-exponential*), *the compressing exponent* β smaller than 2 but greater than 1 in Eq. (1), often averaged for different jammed systems around $\beta \approx 3/2$ [1], is a direct

* Corresponding author at: Jan Dlugosz University in Czestochowa, 13/15, Armii Krajowej str., Czestochowa 4220, Poland.
E-mail address: olehshpotyuk@yahoo.com (O. Shpotyuk).

https://doi.org/10.1016/j.chemphys.2017.12.020
0301-0104/

indicative of *a wide distribution of ballistic relaxation times* [1,4]. Thus, in equilibrium high-temperature over-T_g state, such systems obey *slower-than-exponential* SER kinetics with $\beta \sim 0.9 < 1$, while in low-temperature under-T_g state, they fall out of equilibrium demonstrating *faster-than-exponential* CER kinetics with shape parameter $\beta \sim 1.3 > 1$ [4].

This *equilibrium* versus *out-of-equilibrium dynamical crossover* in some metallic glasses like $Mg_{65}Cu_{25}Y_{10}$ [4] or $Zr_{67}Ni_{23}$ [5] in a vicinity of their glass transition temperature T_g can be well fitted exploring Eq. (1) as *unified master SER-to-CER equation* with universal shape parameters β attaining discrete values above and below unity in dependence on temperature (meaning temperature-governed *SER-to-CER crossover*). Noteworthy, in dependence on structural dispersivity, many of jammed systems such as polymer nanocomposites [10,11] or nanoparticles suspended in supercooled glass-forming liquids [12,13] obey dynamical behavior in more equilibrium state in respect to single exponential function ($\beta = 1.0$) rather than SER.

Detailed dynamics study of some diffusion-prone problems such as protein folding (exemplified by photo-switchable α-helix [16,17] or Go-like protein models [18,19]) allows to identify experimental measuring conditions, under which the tested diffusion kinetics is transformed from SER with $0 < \beta < 1$ to CER with $\beta > 1$. Such *SER-to-CER crossover* was shown to be character for strong perturbation in a system from equilibrium due to experiments performed in a so-called *folding direction*, when system occurs under the action of strong *driving force* allowing *downhill scenario* between rugged energy surface of initial (unfolded) and deeper (folded) state [17,18].

Other examples of hard jammed systems, which demonstrate reach diversity in their equilibrium and non-equilibrium DR kinetics are screen-printed structures formed of nanoinhomogeneous spinel $(Cu,Ni,Co,Mn)_3O_4$ ceramics and conductive Ag- or Ag-Pd-alloyed layers with metallic component (typically Ag) of different migration ability [20–22]. This work is aimed to specify the SER-to-CER crossover observed in thermally-induced electrical DR processes in one of such substances based on spinel $Cu_{0.1}Ni_{0.1}Co_{1.6}Mn_{1.2}O_4$ ceramics.

2. Materials and methods

2.1. Materials preparation

Analytical description of thermally-induced electrical DR kinetics will be developed for bilayer heterostructures of spinel $Cu_{0.1}Ni_{0.1}Co_{1.6}Mn_{1.2}O_4$ ceramics and different conductors prepared by conventional screen-printing route.

The $Cu_{0.1}Ni_{0.1}Co_{1.6}Mn_{1.2}O_4$ ceramics were synthesized by sintering, using reagent grade Cu carbonate hydroxide and Ni, Co, Mn carbonate hydroxide hydrates as was described in more details elsewhere [21–24]. Because of high sintering temperature (1200 °C), the ceramics composed preferentially of spinel phase can be considered as representative of chemical system possessing pronounced nanostructural inhomogeneities due to a wide range of crystalline grains, intergranual boundaries and inner pores [21]. For degradation testing, the samples of bulk-sintered ceramics $Cu_{0.1}Ni_{0.1}Co_{1.6}Mn_{1.2}O_4$ were prepared with flat electrodes fired from Ag paste at 850 °C.

The thick-film samples for this research were made by subsequent stages of paste preparation, screen printing and firing. The paste was prepared by mixing powders of basic spinel $Cu_{0.1}Ni_{0.1}Co_{1.6}Mn_{1.2}O_4$ ceramics with special МБ-60 glass, Bi_2O_3 (used as inorganic binder), organic vehicle and pine oil, taken in a ratio of 72.8:2.9:2.9:17.7:3.7 [21]. The paste was printed on alumina substrates (Rubalit 708S) with conductive layer of Ag or Ag-Pd alloy (fritted as 4:1 Ag/Pd) printed from C1216 paste (Heraeus Precious Metals, GmbH & Co. KG, Hanau, Germany) using a manual device equipped with a steel screen. In final, the thick-film structures were fired at 850 °C.

The prepared bulk-ceramics and thick-film spinel-metallic systems were subjected to degradation testing under prolonged storage at the elevated temperature of 170 °C within a sequence of several time steps lasting 4–500 h. To determine the finalized DR kinetics for each thick-film sample, the cycles of more than 10 separate measurements at different degradation durations were performed. The results of aging tests were controlled by *relative resistance drift* (RRD), i.e. changes in electrical resistance of spinel-metallic system $y = \Delta R/R_0$ detected under normal conditions (25 °C), the confidence interval in the RRD measuring error-bar being ±0.2%. Additional deviations in some points were allowed due to faults in an exact reproduction of DR cycles in multiple sample-to-sample measurements (cooling regime from aging temperature, influence of environment, humidity, etc.). Statistical analysis testified these factors introduced an additional error of about ±0.2% in the measured $y = \Delta R/R_0$ values. So the overall uncertainties in the electrical measurements within this ageing protocol did not exceed ±(0.4–0.5)%.

2.2. Mathematical modelling procedure

The first step in an adequate analytical description of DR kinetics is grounded on preliminary approach, separating mathematical solutions for RRD ($\eta = \Delta R/R_0$) in general differential equation taken as [20]:

$$\frac{d\eta}{dt} = -\lambda \eta^{\alpha} t^{\gamma}, \tag{2}$$

where the power indexes α and γ, as well as λ coefficient ($\lambda \neq 0$) are material-related constants.

The fitting parameters for typical relaxation functions (RFs) derived as solutions of this Eq. (2) were calculated so to minimize mean-square deviation *err* between experimental points and this RF. As was pointed out in [21,22], there are five RFs, representing different partial solutions of Eq. (2) in dependence on α and γ variables, these solutions being gathered in Table 1.

In case of $\alpha = 1$ and $\gamma = 0$, we have a well known monomolecular DR kinetics with RF-1, expressed by simple exponential dependence on time *t*. This case is typical for multi-well systems possessing high inter-well barrier [16,17].

If the degradation is caused by recombination of specific defect pairs, the governing kinetics is defined by bimolecular RF-2 corresponding to $\alpha = 2$ and $\gamma = 0$. Such RD processes are often occurs in irradiated substances due to post-irradiation recombination of defects of opposite nature, such as vacancies and interstitials, electrons and holes, over- and under- coordinated atoms, etc. [25]. Sometimes, when overall relaxation process can be decomposed on separate contributions from different defects, the observed power-law decay behavior can be also well explained in term of bimolecular kinetics [25].

The exact solution of Eq. (2) at $\gamma = 0$ gives the partially-generalized RF-3, which exhibits character "stretched" behavior owing to the α-th-order kinetics of degradation. This RF is often used to describe post-irradiation thermal effects in oxide glasses [25].

In case of $\alpha = 1$ and $\gamma \neq 0$, the relaxation process is described by unified non-exponential RF-4, typical for non-barrier multi-well systems, which can be presented in dependence on β values by SER ($0 < \beta < 1$) or CER ($\beta > 1$) functional. The former (the KWW functional) represents the equilibrium case without downhill driving force, which is most adequate to describe structural, mechanical and electrical relaxation in a large number of disordered solids

Table 1
Numerical solutions of general differential Eq. (2) and their physical relevance for decaying kinetics ($t \to 0 \Rightarrow \eta \to 0$; $t \to \infty \Rightarrow \eta \to -\eta_0$).

DR equation	The RFs as direct solutions of general DR differential Eq. (2)		
	Type	Parameterization	Characterization
$\frac{d\eta}{dt} = -\lambda\eta^{\alpha}t^{\gamma}$ ($\alpha \neq 0$, $\gamma \neq 0$)	$\eta(t) \sim \left(1 + \left(\frac{t}{\tau}\right)^{\beta}\right)^{-\gamma}$	$\tau = \left(\frac{1+\gamma}{\lambda\cdot(\alpha-1)}\right)^{\frac{1}{1+\gamma}}$ $\alpha \neq 1, \gamma \neq -1$ $\beta = 1 + \gamma$ $r = \frac{1}{\alpha-1}$	Fully-generalized RF-5: general description of DR kinetics irrespectively to the microstructure specificity of the system
$\frac{d\eta}{dt} = -\lambda\eta$ ($\alpha = 1$, $\gamma = 0$)	$\eta(t) \sim exp(-\frac{t}{\tau})$	$\tau = \frac{1}{\lambda}$	Monomolecular RF-1: single exponential DR kinetics in multi-well systems possessing high barrier
$\frac{d\eta}{dt} = -\lambda\eta^{2}$ ($\alpha = 2$, $\gamma = 0$)	$\eta(t) \sim (1 + \frac{t}{\tau})^{-1}$	$\tau = \frac{1}{\lambda}$	Bimolecular RF-2: DR kinetics caused by recombination of pairs of opposite-type centers
$\frac{d\eta}{dt} = -\lambda\eta^{\alpha}$ ($\alpha \neq 0$, $\gamma = 0$)	$\eta(t) \sim (1 + \frac{t}{\tau})^{-\beta}$	$\tau = \frac{1}{\lambda}(\alpha - 1)$, $\alpha \neq 1$, $\beta = \frac{1}{\alpha-1}$	Partly-generalized RF-3: "glass"-type kinetics exhibited stretched behavior owing to standard α-th order DR rate dependence
$\frac{d\eta}{dt} = -\lambda\eta t^{\gamma}$ ($\alpha = 1$, $\gamma \neq 0$)	$\eta(t) \sim exp\left[-\left(\frac{t}{\tau}\right)^{\beta}\right]$	$\tau = \frac{1+\gamma}{\lambda}$, $\gamma \neq -1$, $\beta = 1 + \gamma$	Unified non-exponential RF-4 for non-barrier multi-well systems without downhill driving force in an equilibrium (the SER kinetics with $0 < \beta < 1$) or with strong downhill driving force under substantial perturbation from an equilibrium (the CER kinetics with $\beta > 1$)

[26]. The latter is proper to non-equilibrium systems under strong downhill driving force such as photo-switchable α-helix [16,17].

Finally, the exact solution of Eq. (2) with arbitrary non-zero α and γ parameters can be presented by fully-generalized RF-5, which is most trivial one for DR kinetics description from a point of maximal number of fitting parameters.

The formalism of RF-1 – RF-2 – RF-3 – RF-4 – RF-5 consideration (the RFs are listed in Table 1) can be applied to select the best functional describing the probed DR kinetics in terms of minimal mean-square deviation between experimentally measured points (control parameter η) and chosen modelling curve.

3. Results and discussion

3.1. Thermally-induced DR kinetics in bulk-sintered spinel-metallic system

The bulk-sintered $Cu_{0.1}Ni_{0.1}Co_{1.6}Mn_{1.2}O_4$ ceramics with flat electrodes fired from Ag paste show positive response on thermally-induced DR testing, reaching RRD $y = \Delta R/R_0 = 6–7\%$ in near-saturation regime after 400–500 h exposure under 170 °C (Fig. 1). This type of DR dependence is also character for other bulk-ceramics $(Cu,Ni,Co,Mn)_3O_4$ spinels as originated from complicated intrinsic (non-diffusing) processes, evolving thermally-induced cation redistribution and interphase mass-exchange in ceramics grains [27]. This DR kinetics was examined through RFs (Table 1), the results of such parameterization being gathered in Table 2.

It is obvious most adequate description of the observed DR kinetics (Fig. 1) is achieved with a help of SER function (RF-4 in Table 1) due to lowest *err* and only three fitting parameters used in Eq. (2), which is comparable to the results of full-generalized RF-5 with four fitting parameters. The relatively low value of stretching fractional exponent β close to 0.29 testifies in a favor of strong non-exponentionality in the studied system, which is characteristic attribute of structurally-dispersive media [28]. This conclusion is also concomitant with results of other RFs testing (see Table 2), where monomolecular RF-1 proper to barrier-type multi-well systems and bimolecular RF-2 have only worse fitting goodness, but partly-generalized RF-3 describing character "glass" power-type stretched kinetics is in a more close relevance.

Thus, the SER kinetics with positive RRD response on thermally-induced DR testing dominates in bulk-ceramics $Cu_{0.1}Ni_{0.1}Co_{1.6}Mn_{1.2}O_4$ samples with Ag conductive layer, provided all phases of the basics ceramics formed during sintering are equivalent in their origin.

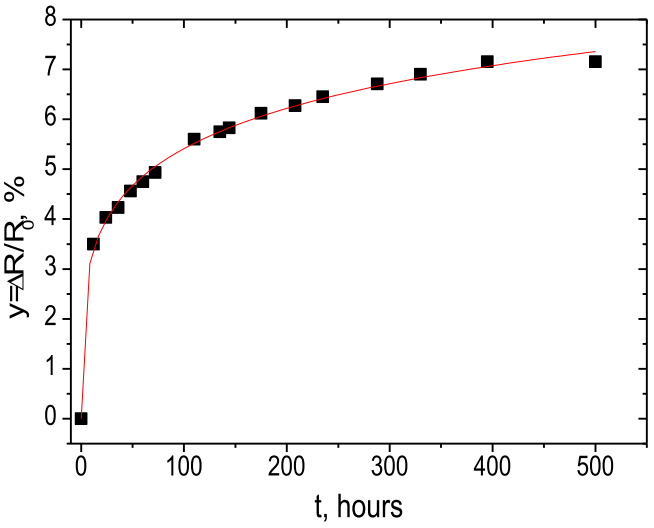

Fig. 1. Thermally-induced (170 °C) relative resistance drift ($\Delta R/R_0$) in bulk-sintered $Cu_{0.1}Ni_{0.1}Co_{1.6}Mn_{1.2}O_4$ spinel ceramics with Ag conductive layer.

3.2. Thermally-induced DR kinetics in spinel-Ag-Pd screen-printed structures

The intrinsic thermally-induced structure-modification processes in $Cu_{0.1}Ni_{0.1}Co_{1.6}Mn_{1.2}O_4$ ceramics becomes inessential in spinel-metallic screen-printed structures. Thus, in $Cu_{0.1}Ni_{0.1}Co_{1.6}Mn_{1.2}O_4$ spinel-Ag-Pd system, the under-barrier diffusion prefers due to metallic conductor penetration in glass-filled intergranual space of ceramics, as it was convincingly revealed from scanning electron microscopy (SEM) with energy-dispersive X-ray (EDX) microanalysis [20,22]. This process results in negative RRD response, showing monotonically decaying tendency in respect to SER function (RF-4 in Table 1) given by master Eq. (1) with stretching exponent $\beta \sim 0.58$ and effective time constant $\tau \sim 32$ h (see Table 3), that is reflected by curve 1 (square-black points) in Fig. 2a. This type of non-exponential kinetics can be also well depicted by line 1 crossing IV-VIII octants in the linearized coordination plane of $\ln(1/y) = f(t/\tau)$ variables shown on Fig. 2b. This linearized form of kinetics presentation is very useful in accurate determination of the shape parameter β, which is numerically equal to the line slope [29–31].

The parameterization of this diffusive-governed kinetics with other RFs listed in Table 1 is ineffective, especially for single-exponential RF-1 in view of obviously worse fitting goodness (compare

Table 2
Parameterization of thermally-induced (T = 170 °C) RRD ($y = \Delta R/R_0$) kinetics in bulk $Cu_{0.1}Ni_{0.1}Co_{1.6}Mn_{1.2}O_4$ spinel ceramics (effects of metallic contacts are excluded).

RFs	*err*	*a*,%.	*τ*, *h*	*β*	*r*
RF-1	0.40	6.6	35	–	–
RF-2	0.13	7.3	25	–	–
RF-3	0.05	10.0	5	0.27	–
RF-4	0.02	10.9	360	0.29	–
RF-5	0.03	10.0	150	0.90	0.30

Table 3
Parameterization of thermally-induced (T = 170 °C) RRD ($y = \Delta R/R_0$) kinetics in screen-printed $Cu_{0.1}Ni_{0.1}Co_{1.6}Mn_{1.2}O_4$ spinel with conductive Ag-Pd layers.

RFs	*err*	*a*, %	*τ*, *h*	*β*	*r*
RF-1	0.22	6.9	22.5	–	–
RF-2	0.06	7.8	17.4	–	–
RF-3	0.04	10.6	5.2	0.32	–
RF-4	0.05	7.8	32.3	0.58	–
RF-5	0.05	9.3	12.5	0.81	0.66

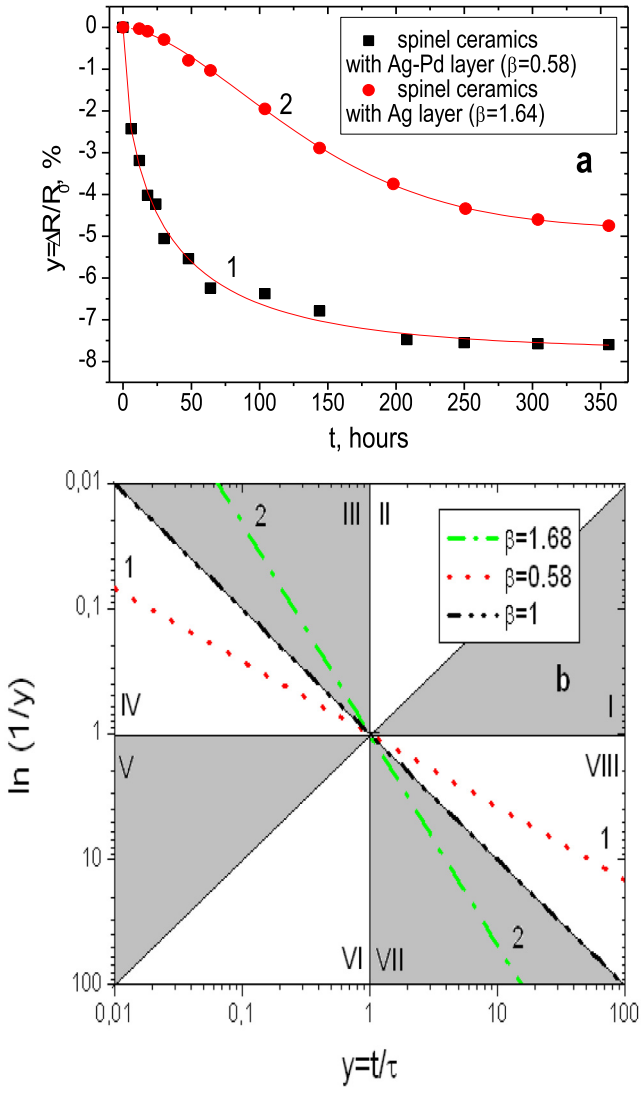

Fig. 2. Kinetics presentation of negative RRD ($y = \Delta R/R_0$) under storage at 170 °C in screen-printed $Cu_{0.1}Ni_{0.1}Co_{1.6}Mn_{1.2}O_4$ spinel with Ag-Pd (1) and Ag (2) conductive layers in the form of $y = f(t)$ dependence (a) and linearized $\ln(1/y) = f(t/\tau)$ presentation (b).

err values in Table 3). Good fitting with "glass"-type RF-3 testifies in a favor of essential power dependence in the DR rate for this kinetics (like in the previous case of intrinsic structure-modification processes in this $Cu_{0.1}Ni_{0.1}Co_{1.6}Mn_{1.2}O_4$ spinel ceramics).

As it follows from Fig. 2, the negative RRD quickly saturates with conductive material penetrating into $Cu_{0.1}Ni_{0.1}Co_{1.6}Mn_{1.2}O_4$ spinel ceramics ($y = \Delta R/R_0 = -7.5\%$). Under these conditions, the Ag-Pd alloy behaves as "cumulative" diffusing agent with a depressed ability of Ag migration. As a result, the DR diffusive process attains strong tendency to yield the SER kinetics.

3.3. Thermally-induced DR kinetics in spinel-Ag screen-printed structures

In contrast, with changing in the conductive material of electrical contacts (i.e. under transition to $Cu_{0.1}Ni_{0.1}Co_{1.6}Mn_{1.2}O_4$ spinel-Ag screen-printed system), the DR kinetics drastically changed attaining an obvious faster than exponential (super-exponential) CER character with over-unity compressibility index $\beta = 1.68$ and time constant τreaching ~154 h (Table 4), depicted by curve 2 (circle-red points) in Fig. 2a. In the coordination plane of $\ln(1/y) = f(t/\tau)$ variables, this kinetics can be simply linearized as it shown by straight line 2 crossing III-VII octants with slope numerically equals to $\beta \sim 1.68$. Noteworthy, in respect to estimated least-square fit goodness (*err* values in Table 4), the tested CER kinetics is far from single-exponential one (RF-1 in Table 1), as well as "glass"-type and bimolecular kinetics (RF-3 and RF-2 in Table 1, respectively).

The SEM-EDX study of Ag distribution profiles in fresh cut-sections between contacting spinel and Ag layers performed before and after degradation testing [20–22] show essential Ag penetration deeply into $Cu_{0.1}Ni_{0.1}Co_{1.6}Mn_{1.2}O_4$ ceramics. The metallic Ag appears in the regions of ceramics adjusted just to conductor contact, as well as in more extended deep region of ceramics grains (over near-micron sizes). In this case, we deal with both under-barrier Ag diffusion in inter-granular glass-filled space, and over-barrier Ag diffusion in grains interior, resulting in diffusive-governed CER kinetics of negative RRD due to master Eq. (1) with fractional exponent $\beta > 1$. So we conclude that if Ag penetration is not inhibited in ceramics by Pd addition, as for $Cu_{0.1}Ni_{0.1}Co_{1.6}Mn_{1.2}O_4$ thick films with contacts made of pure screen-printed Ag layers, the kinetics of the resulting diffusive process is principally changed to CER. The overall diffusion-limited relaxation in the studied

Table 4
Parameterization of thermally-induced (T = 170 °C) RRD ($y = \Delta R/R_0$) kinetics in screen-printed $Cu_{0.1}Ni_{0.1}Co_{1.6}Mn_{1.2}O_4$ spinel with conductive Ag layers.

RFs	*err*	*a*,%	*τ*, *h*	*β*	*r*
RF-1	0.06	6.9	279	–	–
RF-2	0.07	11.3	444	–	–
RF-3	0.08	8.3	1014	3.07	–
RF-4	0.001	4.8	154	1.68	–
RF-5	0.002	5.1	251	1.82	2.73

system occurs as two-step penetration of conductive agent (Ag) into a spinel ceramics body.

As to driving mechanisms responsible for CER kinetics parameterized in Table 3, it is worth mentioning very close similarity in compressing exponent β approaching ~3/2, like in many other out-of-equilibrium systems. Thus, in fractal colloidal gels with $\beta \sim 1.5$, the CER-driving mechanism is ascribed to deformations of elastic network due to the syneresis of the gels [7,8]. In concentrated emulsions and lamellar gels (where β also approaches ~1.5), they are related to collapse of very heterogeneous initial distribution of stresses due to soft contacts between near-spherical particles or local topological rearrangements [7]. In micellar polycrystals with $\beta \cong 1.3–1.7$ [7], the CER behavior of dynamic structure factor is supposed to be attributed to the rearrangement of polycrystal texture, i.e. elastic relaxation of topological defects like dislocations and/or grain boundaries. In polymer nanocomposites such as alumina Al_2O_3 [10] or gold Au nanoparticles [11] embedded in PMMA (polymethylmethacrylate), a faster over-exponential kinetics with $\beta > 1$ (but less than 2) was caused by relaxation of internal stress fields locally developed in these soft glassy systems due to poor wetting of nanoparticle-PMMA interface possibly with holes around these nanoparticles. This CER kinetics was also detected in hard out-of-equilibrium systems such as metallic glasses [14,15], where it was ascribed to ballistic-like hopping motion due to internal stress relaxation. Undoubtedly, these examples testify in a favor of close similarity in their CER-driving mechanisms where out-of-equilibrium stress relaxation plays a governing role.

3.4. SER-to-CER crossover in thermally-induced DR kinetics in spinel-metallic structures

Thus, the thermally-induced DR kinetics probed by RRD ($y = \Delta R/R_0$) in different structurally-dispersive systems composed of bulk-ceramics or screen-printed $Cu_{0.1}Ni_{0.1}Co_{1.6}Mn_{1.2}O_4$ spinel compound with conductive Ag or Ag-Pd layered electrodes obey an obvious non-exponential form, which can be parameterized in respect to master Eq. (1).

Within free energy landscape model like that, explaining the protein folding dynamics [16–19], this situation can be imagined as time evolution of multi-well system between two largely flat metabasins A (an analog of unfolded state) and B (an analog of folded state) without a dominant barrier (Fig. 3). The both metabasins are rugged in respect to a large amount of local states (separate basins) reflecting the nanoinhomogeneity of basics structurally-dispersive ceramics.

In general, this nanoscale inhomogeneity is responsible for non-exponential thermally-induced DR kinetics in *bulk-sintered spinel-metallic systems*, where diffusion-limited processes are inessential in view of short penetration depth of Ag into $Cu_{0.1}Ni_{0.1}Co_{1.6}Mn_{1.2}O_4$ ceramics body. Under such conditions, the intrinsic thermally-induced structure-modification processes, such as cation redistribution and/or interphase mass-exchanging [27], attain a high significance leading to positive RRD governed by slower-than-exponential SER kinetics with β~0.29. As it follows from a great number of models for DR kinetics in

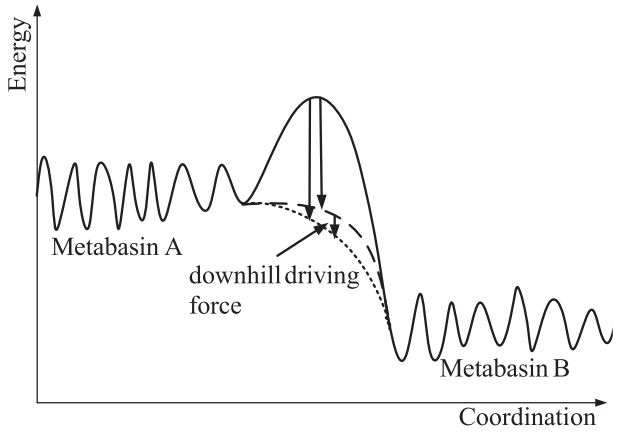

Fig. 3. Fragment of free energy landscape of non-barrier multi-well system exemplified by spinel-conductor screen-printed structure illustrating strong downhill scenarios for DR kinetics due to essential Ag migration inside ceramics (the CER kinetics is observed under substantial perturbation from an equilibrium resulting from disappearing of inter-well barrier denoted by dotted line between two intermediate states composed by A and B metabasins).

$(Cu,Ni,Co,Mn)_3O_4$ ceramics [28], the stretching exponent β reflects difference in their dispersivity, defined by constitution of crystalline grains and intrinsic phase decomposition, the factors which are highly sintering-dependent [23,24].

In *screen-printed spinel-metallic systems*, the DR behavior is principally changed, being governed by external diffusion-type processes related to diffusant penetration into ceramics. In this case, the system evolves between A and B metabasins without free-energy barrier (Fig. 3). So the non-exponentionality in respect to master Eq. (1) will further dominate in the RRD kinetics, but its occurrence is strongly defined by extrinsic nanoinhomogeneities introduced in a system due to diffusant. The governing kinetics attains an obvious sub-exponential form (SER kinetics) with below-unity stretching exponent $0 < \beta < 1$, provided the system behaves as in equilibrium. This situation corresponds to one-stage diffusion process in structurally dispersive media like screen-printed spinel $Cu_{0.1}Ni_{0.1}Co_{1.6}Mn_{1.2}O_4$ ceramics, where Ag migration is significantly inhibited by Pd addition due to conductive Ag-Pd alloy. In such systems, there are no any driving forces able to accelerate diffusion-limiting DR kinetics.

Under Ag penetration deeply into spinel ceramics, as for thick-film systems with Ag-layered electrodes, the resulting DR kinetics drastically changes, attaining features of two-step diffusing process governed by CER function with over-unity $\beta \sim 1.68$ compressibility index. The Ag atoms can migrate in spaces between crystalline grains filled with glass binder, this first-stage of diffusion-related process being quickly saturated via SER kinetics. Microscopically, this process can be ascribed to continuous generation and accumulation of Ag ions, their further recharging into metallic silver followed by formation of cloud-like layers or dendritic migration outgrowths [31–33]. Whichever the case, by penetrating intergranual spaces in thick-film spinel body, the Ag ions attain a possibility for further migration into bulk grains composed of $Cu_{0.1}Ni_{0.1}Co_{1.6}Mn_{1.2}O_4$ spinel, thus leading to

second-stage diffusion. In such a way, the ceramics material evolving crystalline $Cu_{0.1}Ni_{0.1}Co_{1.6}Mn_{1.2}O_4$ grains, intergranual barriers and structurally-intrinsic pores forms a specific hard jammed system, where strong downhill scenarios appear as an input from additional Ag penetration into ceramics. Therefore, the overall diffusion-limited DR process in the studied thick-film system occurs as two-step diffusant (Ag) penetration into ceramics. Within free-energy landscape shown in Fig. 3, this process can be conditionally depicted as decreasing tendency in a path between A and B metabasins (downhill driving force).

In terms of heterogeneity [34], the non-exponential (SER or CER) DR kinetics can be described by heterogeneity factor h (which is inverse stretching factor $1/\beta$), giving the degree of system deviation from homogeneous single-exponential RF-1. This parameter for SER kinetics (Fig. 2a, curve 1) is significantly greater unity ($h = 1.72$), reflecting complex "glassy"-type processes dominated by multiple local minima. For CER kinetics (Fig. 2a, curve 2), the heterogeneity factor $h = 0.61$ corresponds to "non-glassy"-type kinetics (which is strongly non-exponential) in Ag penetrating into ceramics.

Hence, in fact, the SER-to-CER kinetics crossover appears in screen-printed ceramics-conductor systems due to strong structural perturbation from equilibrium caused by diffusing agent (Ag). In many substances prepared in out-of-equilibrium state by quenching from a liquid, the internal stresses are inevitably built in at the jamming transition [7,8]. These stresses relaxing at further experimental conditions serve as a source for unusual CER behavior. In case of our thick films, this type of relaxation dominates under a condition of dynamic nanoinhomogeneities caused by Ag penetration deep into ceramics bulk. This diffusive process is only the initiating stage of the overall relaxation tending a system towards equilibrium, while the final ultraslow stage attains faster than exponential CER form. The relaxation of internal stresses has no direct relation to this first-stage diffusive motion, being principally different in its origin. Thus, the driving microstructure mechanisms responsible for CER are known to be related to stresses collapse due to soft contacts between spheres (as in case of concentrated emulsions and lamellar gels), local topological rearrangements (as in foams), elastic relaxation of topological defects like dislocations or grain boundaries (as for micellar crystals), etc. [7]. Typically, such structural rearrangements occur on length scales of over-microns distances [7]. Thus, it should be admitted reasonably that Ag atoms penetrating $Cu_{0.1}Ni_{0.1}Co_{1.6}Mn_{1.2}O_4$ ceramics, mainly in a vicinity of intergranual boundaries, create specific micron-sized bridges between grains, increasing electrical conductivity of a whole system.

4. Conclusions

Thermally-induced DR kinetics probed by relative electrical resistance drift in structurally-dispersive systems composed of bulk-ceramics or screen-printed $Cu_{0.1}Ni_{0.1}Co_{1.6}Mn_{1.2}O_4$ spinel compound with conductive Ag or Ag-Pd layered electrodes is shown to obey an obvious non-exponential form. Two different types of kinetics are detected for the same thick-film ceramics in dependence on supplied metallic contacts. If Ag migration is inhibited by Pd addition due to conductive Ag-Pd alloy, the governing kinetics attains a stretched exponential form with stretching exponent $\beta = \sim 0.58$ typical for one-stage diffusion in structurally dispersive media. Under Ag penetration into thick-film body, as for thick-films supplied by Ag contacts, the kinetics drastically changes, attaining compressed-exponential form with shape index $\beta = 1.68$. The resulting kinetics in this case is though to be attributed to two-step diffusing process originated from Ag penetration deep into spinel $Cu_{0.1}Ni_{0.1}Co_{1.6}Mn_{1.2}O_4$ ceramics.

Acknowledgements

The authors acknowledge support from Science and Technology Center in Ukraine under STCU Project No 6371. OSh acknowledges support of research project from German Academic Exchange Service (DAAD – Deutscher Akademischer Austauschdienst).

References

[1] R. Kohlrausch, Theorie des Elektrischen Rückstandes in der Leidener Flasche, Pogg. Ann. Phys. Chem. 91 (1854) 179–214.
[2] G. Williams, D.C. Watts, Non-symmetrical dielectric relaxation behaviour arising from a simple empirical decay function, Trans. Farad. Soc. 66 (1970) 80–85.
[3] R.G. Palmer, D.L. Stein, E. Abrahams, P.W. Anderson, Models of hierarchically constrained dynamics for glassy relaxation, Phys. Rev. Lett. 53 (1984) 958–961.
[4] J. Klafter, M.F. Shlesinger, On the relationship among three theories of relaxation in disordered systems, Proc. Natl. Acads. Sci. U.S.A. 83 (1986) 848–851.
[5] J.C. Phillips, Stretched exponential relaxation in molecular and electronic glasses, Rep. Prog. Phys. 59 (1996) 1133–1207.
[6] L.C.E. Struik, Physical Ageing in Amorphous Polymers and Other Materials, Elsevier, New York, 1978.
[7] L. Cipelletti, L. Ramos, S. Manley, E. Pitard, D.A. Weitz, E.E. Pashkovski, M. Jahnsson, Universal non-diffusive slow dynamics in aging soft matter, Faraday Discuss. 123 (2003) 237–251.
[8] L. Cipelletti, S. Manley, R.C. Ball, D.A. Weitz, Universal aging features in the restructuring of fractal colloidal gels, Phys. Rev. Lett. 84 (2000) 2275–2278.
[9] P. Ballesta, A. Duri, L. Cipelletti, Unexpected drop of dynamical heterogeneities in colloidal suspesions approaching the jamming transition, Nat. Phys. 4 (2008) 550–554.
[10] R.A. Narayanan, P. Thiyagarajan, S. Lewis, A. Bansal, L.S. Schadler, L.B. Lurio, Dynamics and internal stress at the nanoscale related to unique thermomechanical behavior in polymer nanocomposites, Phys. Rev. Lett. 97 (2006) 075505-1–075505-4.
[11] S. Srivastava, A.K. Kandar, J.K. Basu, M.K. Mukhopathyay, L.B. Lurio, S. Narayanan, S.K. Sinha, Complex dynamics in polymer nanocomposites, Phys. Rev. E 79 (2009) 021408-1–021408-7.
[12] C. Caronna, Y. Chushkin, A. Madsen, A. Cupane, Dynamics of nanoparticles in a super cooled liquid, Phys. Rev. Let. 100 (2008) 055702-1–055702-4.
[13] H. Guo, G. Bourret, M.K. Corbierre, S. Rucareanu, R. Bruce Lennox, K. Laaziri, L. Piche, M. Sutton, J.L. Harden, R.L. Leheny, Nanoparticle motion within glassy polymer melts, Phys. Rev. Lett. 102 (2009) 075702-1–075702-4.
[14] B. Ruta, Y. Chushkin, G. Monaco, L. Cipelletti, E. Pineda, P. Bruna, V.M. Giordano, M. Gonzalez-Silveira, Phys. Rev. Lett. 109 (2012) 165701-1–165701-5.
[15] B. Ruta, G. Baldi, G. Monaco, Y. Chushkin, Compressed correlation functions and fast aging dynamics in metallic glasses, J. Chem. Phys. 138 (2013) 054508-1–054508-6.
[16] P. Hamm, J. Helbing, J. Bredenbeck, Stretched versus compressed exponential kinetics in α-helix folding, Chem. Phys. 323 (2006) 54–65.
[17] J. Bredenbeck, J. Helbing, J.R. Kumita, G.A. Woolley, P. Hamm, α-Helix formation in a photoswitchable peptide tracked from picoseconds to microseconds by time-resolved IR spectroscopy, PNAS 102 (2005) 2379–2384.
[18] H. Nakamura, M. Sasai, M. Takano, Scrutinizing the squeezed exponential kinetics observed in the folding simulation of an off-lattice Go-like protein model, Chem. Phys. 307 (2004) 259–267.
[19] H.K. Nakamura, M. Sasai, M. Takano, Squeezed exponential kinetics to describe a nonglassy downhill folding as observed in a lattice protein model, Proteins 55 (2004) 99–106.
[20] V. Balitska, O.I. Shpotyuk, On the non-exponential degradation kinetics in functional ceramics, Arch. Mater. Sci. 27 (2006) 189–199.
[21] H. Klym, V. Balitska, O. Shpotyuk, I. Hadzaman, Degradation transformation in spinel-type functional thick-film ceramic materials, Microelectron. Reliab. 54 (2014) 2843–2848.
[22] O. Shpotyuk, M. Brunner, I. Hadzaman, V. Balitska, H. Klym, Analytical description of degradation-relaxation transformations in nanoinhomogeneous spinel ceramics, Nanoscale Res. Lett. 11 (2016) 499-1–499-6.
[23] M. Vakiv, O. Shpotyuk, O. Mrooz, I. Hadzaman, Controlled thermistor effect in the system $Cu_xNi_{1-x-y}Co_{2y}Mn_{2-y}O_4$, J. Eur. Ceram. Soc. 21 (2001) 1783–1785.
[24] O. Shpotyuk, V. Balitska, I. Hadzaman, H. Klym, Sintering-modified Ni-Co-Cu oxymanganospinels for NTC electroceramics, J. Alloys Comp. 509 (2011) 447–450.
[25] D.I. Griscom, M.E. Gingerich, E.J. Friebele, Radiation-induced defects in glasses: origin of power-law dependences of concentration on dose, Phys. Rev. Lett. 71 (1993) 1019–1023.
[26] O.V. Mazurin, Relaxation phenomena in glass, J. Non-Cryst. Solids 25 (1977) 130–169.
[27] M. Vakiv, I. Hadzaman, O. Shpotyuk, O. Mrooz, J. Plewa, H. Altenburg, H. Uphoff, O. Bodak, P. Demchenko, On the role of mass-transfer processes in ageing of manganite electroceramics, J. Eur. Ceram. Soc. 24 (2004) 1277–1280.

[28] O. Shpotyuk, V. Balitska, M. Brunner, I. Hadzaman, H. Klym, Thermally-induced electronic relaxation in structurally-modified $Cu_{0.1}Ni_{0.8}Co_{0.2}Mn_{1.9}O_4$ spinel ceramics, Phys. B 459 (2015) 116–121.
[29] M. Mao, Z. Altounian, Accurate determination of the Avrami exponent in phase transformations, Mater. Sci. Eng. A 149 (1991) L5–L8.
[30] Y. Gueguen, V. Keryvin, T. Rouxel, M. Le Fur, H. Orain, B. Bureau, C. Boussard-Pledel, J.-C. Sangleboeuf, A relashinship between non-exponential stress relaxation and delayed elasticity in the viscoelastic process in amorphous solids: illustration on a chalcogenide glass, Mechan. Mater. 85 (2015) 47–56.
[31] J.C. Lin, J.Y. Chan, On the resistance of silver migration in Ag-Pd conductive thick films under humid environment and applied d.c. field, Mater. Chem. Phys. 43 (1996) 256–265.
[32] Vu. Kim, Silver migration – the mechanism and effects on thick-film conductors, Mater. Sci. Eng. 234 (2003) 1–21.
[33] S. Yanga, J. Wua, A. Chritoua, Initial stage of silver electrochemical migration degradation, Microelectron. Realib. 46 (2006) 1915–1921.
[34] B. Gillespie, K.W. Plaxco, Nonglassy kinetics in the folding of a simple single-domain protein, PNAS 97 (2000) 12014–12019.